International Journal of Geographical Information Science
Vol. 26, No. 4, April 2012, 599–620

Modeling experimental cross-transiograms of neighboring landscape categories with the gamma distribution

Weidong Li[a,b]*, Chuanrong Zhang[b] and Dipak K. Dey[c]

[a]*College of Resource and Environmental Information, Huazhong Agricultural University, Wuhan, China;* [b]*Department of Geography, University of Connecticut, Storrs, CT, USA;* [c]*Department of Statistics, University of Connecticut, Storrs, CT, USA*

(*Received 19 August 2010; final version received 4 July 2011*)

Effectively fitting the major features of experimental transiograms (or variograms) is crucial in characterizing spatial patterns and reproducing them in geostatistical simulations. Landscape patterns usually tend to contain neighboring structures. The experimental cross-transiograms of frequent neighboring landscape categories normally demonstrate apparent peaking features at low lag distances – they first quickly increase to a peak and then gradually flatten out. The flattening process may be smooth or may be through one or more alternate attenuating troughs and peaks. While alternate peaks and troughs may be a reflection of the cyclic occurrence of landscape categories, the single peak or the first peak at low lag section should be a signal of the neighboring structure of two related categories. This is further proved by the peaking features of some idealized transiograms calculated from single-step transition probability matrices. To effectively fit the first peak, especially when it is the single one, we propose using the gamma distribution function and the commonly used variogram models to form additive composite models. Cases of fitting experimental cross-transiograms of landscape data (here soil types and land cover classes) show that the additive gamma-exponential composite model works very well and may closely fit the single-peak features. Although it has multiple parameters to set, model fitting can be performed manually by trial and error. Other two composite models may provide alternatives for fine fitting of the root section (i.e., the left side of the peak). These models may also be applicable to fitting experimental variograms with similar features. We also reintroduce the multiplicative composite hole-effect models proposed for variogram modeling by earlier researchers, and test them on experimental cross-transiograms. It is found that composite hole-effect models are not sufficiently flexible to effectively fit the peak shapes of experimental cross-transiograms of neighboring categories, unless multiple peaks and troughs appear in regular shapes and rhythms.

Keywords: landscape heterogeneity; neighboring categories; transiogram; gamma distribution; spatial metric

1. Introduction

Categorization is a common way used to characterize and map the complex spatial heterogeneity of many spatial phenomena such as various landscapes (Robbins 2001, Hobbs and McIntyre 2004). A categorical (or discrete) spatial variable, which characterizes the

*Corresponding author. Currently affiliated with the University of Connecticut. Email: weidongwoody@gmail.com

ISSN 1365-8816 print/ISSN 1362-3087 online

http://dx.doi.org/10.1080/13658816.2011.603336
http://www.tandfonline.com

spatial heterogeneity of a specific spatial phenomenon (e.g., land use/cover, soil type, lithofacies, pollution grade, land quality grade, wind speed gradient), usually has multiple or a number of categories (or classes). Among the multiple categories of a categorical spatial variable, some may frequently occur as neighbors, that is, they may occur closely in space. When two categories often occur closely, that means they associate with or depend on each other strongly. In this study, we call such two categories *neighboring categories* and their co-occurrence *neighboring structure*. Similar situation also occurs in categorical temporal variables, such as the time series of landscape change. In this paper, however, we focus only on categorical spatial variables.

Because of the complexity of spatial heterogeneity, the intraclass and interclass dependencies (or correlations) among the categories of landscapes are also very complex (Turner 1989, Li and Reynolds 1993a, Pickett and Cadenasso 1995). A variety of spatial metrics, such as the contagion index (Li and Reynolds 1993b, O'Neill *et al*. 1988) and the interspersion and juxtaposition index (McGarigal and Marks 1995), have been proposed to measure the dependencies of categories in landscape ecology in the recent two decades (Riitters *et al*. 1995, Haines-Young and Chopping 1996, Wu *et al*. 2002, Palmer 2004, Dietzel *et al*. 2005, Pijanowski *et al*. 2005, Dendoncker *et al*. 2008). Although single-step transition probabilities have been often used to describe the spatial (or temporal) change of land use/cover patterns (Pontius and Malanson 2005, Geertman *et al*. 2007, Almeida *et al*. 2008), the *transiogram*, which was proposed recently as a spatial measure for categorical data, has its unique merits as a quantitative graphic measure (Li 2006, 2007a), and may serve as a spatial metric for characterizing landscape heterogeneity (Li and Zhang 2011). Transiograms are resolution-free and can indicate spatial (or temporal) auto- and cross-correlation information at different lag distances. Similar to indicator variograms (Deutsch and Journel 1998), which have been often used for categorical data in geostatistics, transiograms measure auto and cross-correlations over a series of lag distances. However, as transition probability diagrams, cross-transiograms are asymmetrical; that means they can be more complex in shape than indicator variograms, which are covariance-based and symmetrical in definition. Also as transition probability diagrams, transiograms are more intuitive and interpretable than indicator variograms (Li 2007a). Thus, a transiogram essentially provides an ideal two-point spatial measure for characterizing complex categorical patterns.

A major use of transiograms is to provide correlation information to geostatistical methods, such as the Markov chain geostatistics (Li 2007b, Li and Zhang 2007), that use transition probabilities with different lags for conducting stochastic simulations of categorical fields. Markov chain geostatistics use Markov chain random field (MCRF) models as local conditional probability estimators and continuous transiogram models as spatial dependency descriptors of categories in geospatial processes. These transiogram models may be fitted mathematical models or interpolated experimental transiograms. Note that although linear interpolation was suggested as a way to obtain continuous transiogram models from experimental transiograms for MCRF simulations, it is only recommended as one alternative under the condition that sample data are sufficient to provide reliable experimental transiograms (Li and Zhang 2010, 2011). Such a simple way may not be applicable to other transition probability-based geostatistical methods such as the transition probability-based indicator geostatistics extended from indicator kriging by Carle and Fogg (1996), and it also eliminates the chance to use expert knowledge in constructing a transiogram model. In addition, even if geostatistical simulation is not conducted, mathematical model fitting of experimental transiograms may still be necessary for using transiograms as independent spatial measures (similar to variograms) to characterize categorical spatial

patterns, because the type and parameters of a mathematical model may be simple indices of spatial patterns. These mean that effective mathematical model fitting of experimental transiograms is crucial to geostatistical simulation and pattern characterization of categorical fields.

To some extent, transiograms are also similar to indicator variograms in shapes. But they have opposite changing directions. While transiograms are always positive, cross indicator variograms between mutually exclusive categories are negative. Quantitative relationships between transiograms (or transition probabilities) and indicator variograms also could be established (Lou 1993, Carle and Fogg 1996). Therefore, the commonly used variogram models, such as the linear, spherical, Gaussian, and exponential models (Goovaerts 1997), can be simply adapted for fitting experimental transiograms (Ritzi 2000, Li 2007a). Experimental auto-transiograms usually have relatively simple shapes and they often tend to be exponential with one or multiple ranges. So it is not difficult to use simple models (e.g., exponential and spherical models) or their linear combinations (i.e., nested models) to fit them. However, experimental cross-transiograms can be very complex in their shapes. A typical special feature is that some experimental cross-transiograms may first have a peak, then gradually flatten out with increasing lag distance (Li 2007a). Such a peak in an experimental cross-transiogram, if close to the origin, typically reflects the frequent neighborship of two categories. Such kind of shapes cannot be captured by the commonly used variogram models or even with their nested structures because these models increase monotonically (Ma and Jones 2001). If there is one or a series of attenuated troughs and peaks following the first peak, dampened hole-effect models may provide a good fit at some situations. However, dampened hole-effect models cannot always fit well, because the periodicity may not be regular, and the peaks (or troughs), particularly the first peak, may be too high (or low) and too wide (or narrow) to fit (Ma and Jones 2001). If there is no trough following the first peak, we find that no existing variogram model can be used to fit such kind of experimental cross-transiograms with a single peak. The problem is that neighborship (or called juxtaposition) is a normal, widely existing situation in categorical spatial variables. Some categories tend to occur together mutually, and some categories tend to occur aside the other categories unilaterally. These situations cause some of the experimental cross-transiograms to have a peak at their low lag sections. To effectively reproduce such kind of categorical patterns in geostatistical simulations or quantitatively characterize them, it is necessary to develop proper transiogram models to fit experimental cross-transiograms with this kind of shapes.

The gamma distribution has the characteristics of first peaking and then flattening out (Rice 1995). Thus, it may provide an essential component in constructing composite transiogram models for fitting the special peaking features. The objectives of this study are: (1) to display the features of experimental transiograms, particularly the peaking features of experimental cross-transiograms of neighboring categories, estimated from different data sets; (2) to suggest a set of composite mathematical models for cross-transiogram modeling based on the gamma distribution; and (3) to demonstrate the fitting effectiveness of the additive gamma-exponential composite model and the multiplicative cosine-exponential composite model to the peaking features of experimental cross-transiograms. The proposed models should also be applicable to fitting experimental variograms with similar features. The rest of this paper is arranged as follows: We first display some experimental transiograms estimated from different data sets and prove the validity of the peaking features appearing on some experimental cross-transiograms using idealized transiograms in Section 2.In Section 3, we focus on exploring the gamma distribution and investigating how to combine the gamma distribution with the commonly used variogram models

to fit the peaking features of experimental cross-transiograms of neighboring categories. Then in Section 4, we introduce hole-effect models and show that some of the experimental cross-transiograms with hole effects may be fitted well by using the existing composite hole-effect models, whereas others may not, due to the limitation of hole-effect models in peak (or trough) heights and widths. Finally, we conclude this paper by recommending the use of additive gamma distribution-based composite models.

2. Features of transiograms

2.1. The concepts of transiograms

The transiogram was proposed mainly as an accompanying spatial measure for the Markov chain geostatistics (Li 2007a, Li and Zhang 2007). Let Z be a categorical variable with n categories, defined in a state space $S = (1, 2, \ldots, n)$, and z be a specific category of Z at a specific location $\mathbf{x}$. A theoretical transiogram is defined as a transition probability function over the lag distance $\mathbf{h}$:

$$p_{ij}(\mathbf{h}) = \Pr(z(\mathbf{x} + \mathbf{h}) = j \mid z(\mathbf{x}) = i) \tag{1}$$

where both j and i represent categories (Li 2006, 2007a). An auto transiogram p_{ii} $(\mathbf{h})$ represents the self-dependence (i.e., auto-correlation) of a single category i, and a cross-transiogram $p_{ij}(\mathbf{h})$ $(i \neq j)$ represents the cross-dependence of category j on category i. Here, category i is called the head class and category j is called the tail class. Note that $p_{ij}(\mathbf{h}) \neq p_{ji}(\mathbf{h})$ usually, because cross-transiograms are asymmetric.

In practice, one can estimate a transiogram directly from sample data by counting the number of transitions from a category to itself or another category over a series of lag distances using the following equation:

$$\hat{p}_{ij}(\mathbf{h}) = \frac{F_{ij}(\mathbf{h})}{\sum_{k=1}^{n} F_{ik}(\mathbf{h})} \tag{2}$$

where $F_{ij}(\mathbf{h})$ represents the number of transitions from category i to category j at the lag distance $\mathbf{h}$, and n is the total number of categories. The lag distance can be absolute distance (e.g., meters or kilometers) or relative distance (e.g., numbers of pixel lengths for raster data). Such a transiogram estimated directly from sample data is called an experimental (or empirical) transiogram, and is usually denoted as $\hat{p}_{ij}(\mathbf{h})$. To acquire reliable experimental transiograms from sparse samples, one needs to set a lag tolerance Δh around each specific lag distance value, which may be decided by users according to the density of samples. If the variable Z is anisotropic, experimental transiograms may have to be estimated directionally with a tolerance angle similar to the estimation of variograms (Deutsch and Journel 1998, p. 49). Experimental transiograms are sequences of discontinuous transition probability values at different lag distances. However, continuous transiograms are needed in geostatistical simulations. Thus, we need to infer continuous transiograms from experimental ones through model fitting or using other ways (e.g., interpolation, expert knowledge). Such continuous transiograms are called transiogram models or model transiograms.

Transiograms are diagrams of transition probabilities with increasing lag distance. If a one-step transition probability matrix (TPM) $\boldsymbol{P}(1) = [p_{ij}\ (1)]$ can be available, one even can directly calculate transiograms from the TPM by its self-multiplication. That is, one

can get n-step transition probabilities from one-step transition probabilities by calculating the following equation:

$$\boldsymbol{P}(n) = [p_{ij}(n)] = [\boldsymbol{P}(1)]^n = [p_{ij}(1)]^n \quad (3)$$

where n refers to the number of spatial steps. A series of transition probabilities from i to j at different spatial steps (i.e., 1, 2, 3, . . ., n steps) form a transiogram with gaps of one-step length. Such a transiogram is called an idealized transiogram because the above calculation equation is based on the first-order stationary Markovian assumption, and transiograms derived as such have idealized shapes. Similarly, if a two-step TPM is available, one can also get a series of transition probabilities at multiple steps such as 2, 4, 6, 8, . . ., $2n$ using the similar way as the above equation. These transition probabilities at different steps can also form transiograms, but with gaps of two-step lengths. Therefore, idealized transiograms are not completely continuous curves.

Because TPMs are not always available (i.e., cannot be accurately estimated from irregular sample data), idealized transiograms are also not always available. Estimated from samples with lag and angle tolerances, single-step transition probability values of experimental transiograms are not accurate in lags and directions. However, because they are all directly estimated from real data without presuming the first-order stationary Markovian assumption, experimental transiograms as visual curves are able to reflect the global characteristics of spatial heterogeneity. Examples in experimental transiograms and idealized transiograms will be given in next subsections.

2.2. *Experimental transiograms*

From our experience, we find that experimental auto-transiograms basically decrease monotonically with increasing lag distance. Although sometimes weak peaks and troughs may appear, they are not obvious, and can be ignored. Thus, they can be fitted easily by the commonly used models such as exponential and spherical models or their nested structures. However, whereas some experimental cross-transiograms have the general monotonic trend with increasing lag distance, others may show apparent peaking features – first quickly increasing to a peak and then gradually flattening out. The flattening process has two different situations: one is a typical monotonic decrease, and the other is a decrease through a series of attenuated troughs and peaks. The latter is similar to the dampened hole-effect feature of some experimental variograms, which has been studied in geostatistics (e.g., Journel and Huijbregts 1978, Ma and Jones 2001, Pyrcz and Deutsch 2003). For the former, we find no literature in geostatistics to mention it in variogram modeling. However, in transiogram modeling, this feature is too outstanding to be ignored.

Figure 1 shows some unidirectional experimental transiograms estimated from a soil map of 9.6 × 9.6 km^2 with 48 soil series, ever used in Li (2007a). It can be seen that the experimental auto-transiograms are relatively simple in shapes compared with the cross ones and tend to be exponential-shaped with multiple ranges or spherical-shaped (Figure 1d). However, as shown in Figure 1a–c, experimental cross-transiograms are far more complex in their shapes: some have peaking features, whereas others do not have. Peaking features are especially outstanding on some transiograms in Figure 1a and b. Such features should not be regarded as dubious signals caused by data problems. Typically, they are reflections of the closely neighboring characteristics of some soilscape categories (i.e., soil types). Interestingly, in Figure 1c we find two cross-transiograms both having a large, wide peak, which occurs some distance away from the origin. Although this also reflects

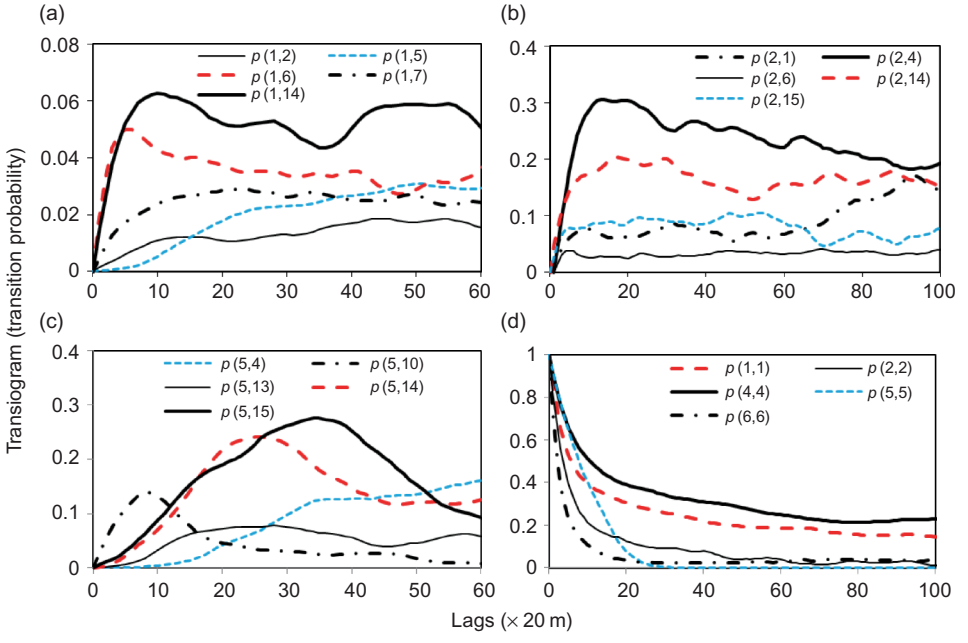

Figure 1. Unidirectional experimental transiograms estimated from a soil map data set along the east-to-west direction. Pixel size is 20 m × 20 m. Here $p(i, j)$ refers to the experimental transiogram $\hat{p}_{ij}(\mathbf{h})$.

the neighborship of the two categories, the two categories are not very close neighbors. No significant cyclic features can be found, although irregular fluctuations do appear on some cross-transiograms.

Not only do the peaking features occur on unidirectional or anisotropic experimental cross-transiograms but they also occur on some omnidirectional experimental cross-transiograms. Figure 2 shows some omnidirectional experimental cross-transiograms estimated from a large sample data set of 12,936-point data, thinned from the soil map used for estimating Figure 1. It is clear that some experimental cross-transiograms reveal the peaking features, with a high or low peak. Changing the lag tolerance from 3 pixel lengths to 6 pixel lengths does not eliminate the peaking features, which means the peaking features of the experimental cross-transiograms are not caused by data noise or errors (Figure 3a). Again, the omnidirectional experimental auto-transiograms are close to be exponential-shaped, but some obviously have multiple correlation ranges (Figure 3b). In addition, experimental transiograms from land cover class data indicate the similar features.

2.3. Idealized transiograms

To further prove that the peaking features appearing on some experimental cross-transiograms are not dubious signals caused by data problems, in Figures 4 and 5 we display some idealized transiograms calculated using one-step TPMs, which are computed from soil and land cover map data. Because map data are exhaustive, we can directly calculate unidirectional one-step TPMs, then further calculate idealized transiograms by self-multiplications of a TPM. It can be seen from Figures 4 and 5 that idealized transiograms have very smooth curves, and some idealized cross-transiograms still have

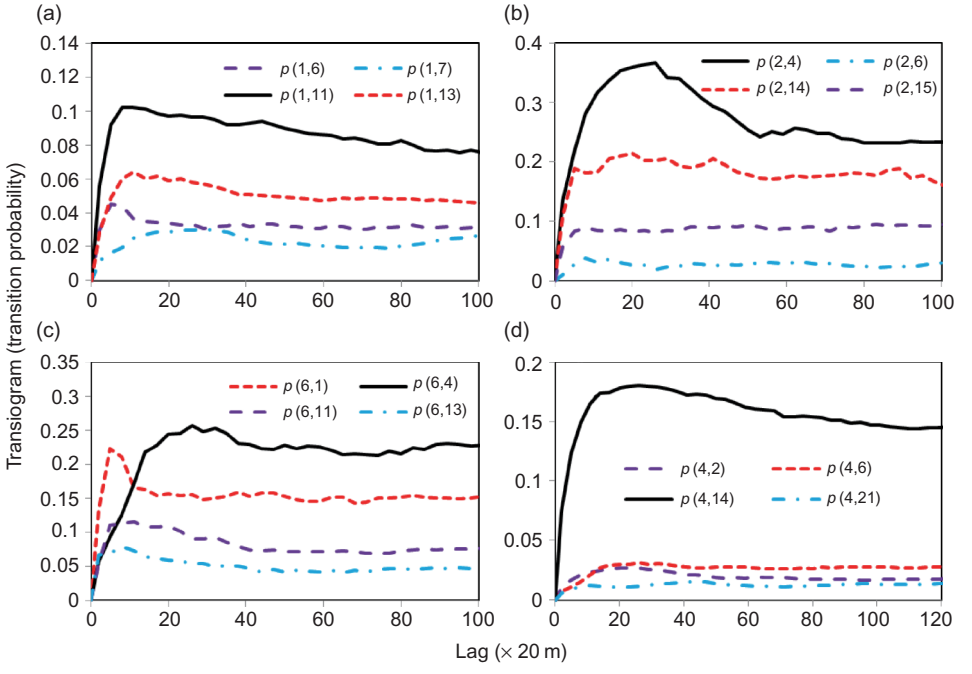

Figure 2. Omnidirectional experimental cross-transiograms estimated from a large soil sample data set of 12,936-point data with a lag tolerance of 3-pixel lengths.

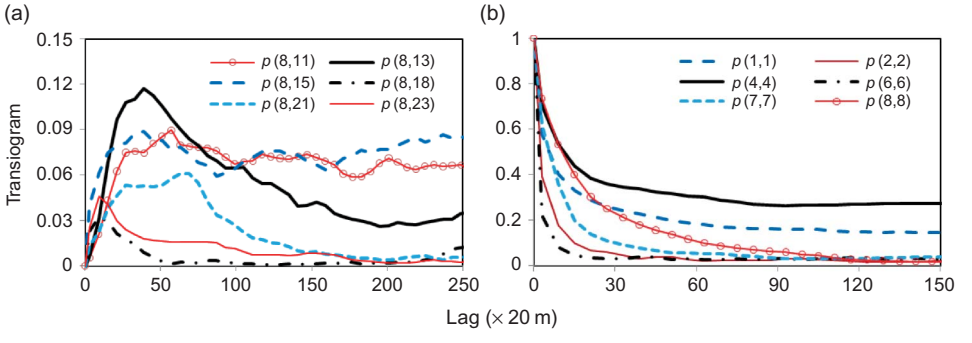

Figure 3. Omnidirectional experimental cross-transiograms estimated from a large soil sample data set of 12,936-point data with a lag tolerance of 6-pixel lengths.

peaking features – first quickly peaking and then flattening out. The difference between idealized and experimental cross-transiograms is that on the idealized cross-transiograms with peaking features, only one single peak appears.

The special characteristics of idealized transiograms are not difficult to understand: They are the reflections of the implicit assumptions behind the calculation method (Equation (3)), which supposes the first-order Markovian assumption and assumes that the data for estimating the single-step transition probabilities are spatially stationary, sufficient, and obtained from an infinitely large area. With such assumptions, any experimental transiogram features, caused by data nonstationarity, data insufficiency, and area limitation, are removed from the idealized ones. Because a marked hole effect (i.e., a series of peaks and

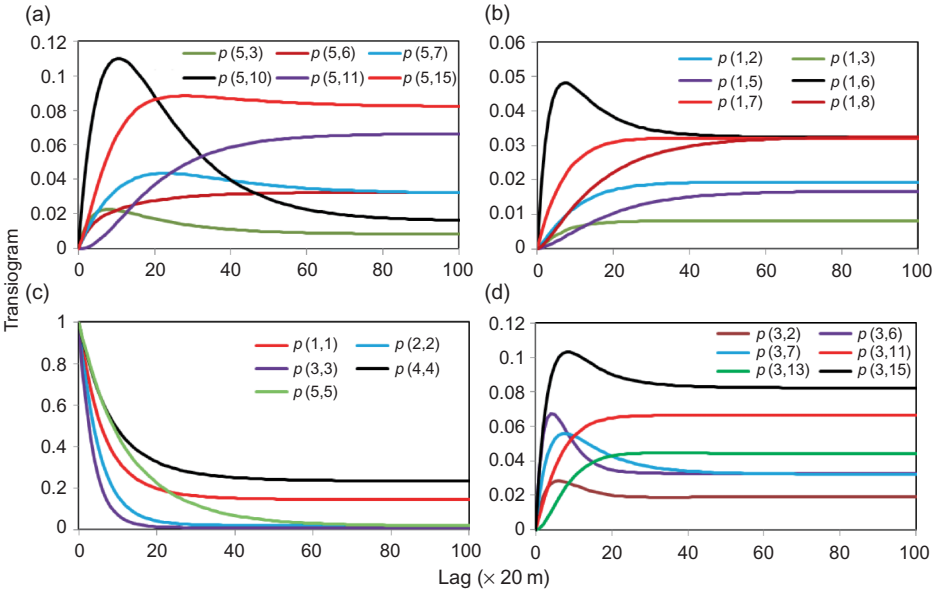

Figure 4. Some idealized transiograms calculated from a unidirectional TPM which is computed from soil map data.

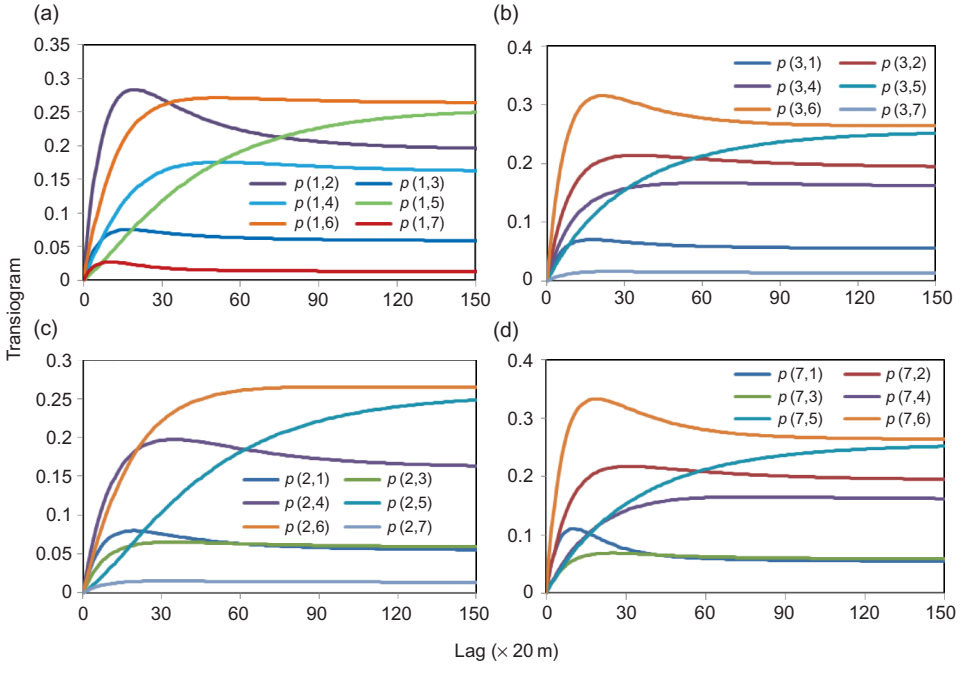

Figure 5. Some idealized cross-transiograms calculated from a four-directional TPM which is computed from land cover map data of seven classes.

troughs) is the reflection of pseudo-periodical occurrences of the neighboring structure of two categories, and the pseudo-periodicity is typically a kind of data nonstationarity, there is no way for multiple peaks and troughs to appear on idealized transiograms. That means no matter how the neighboring structures of two categories are distributed in space – randomly, irregularly, or cyclically – what is reflected on idealized transiograms is just a single smooth peak. Because they are caused by data insufficiency and area limitation (i.e., insufficient data pairs at some lag distances and limited patterns in a study area), irregular fluctuations that generally appear on experimental transiograms do not occur on idealized transiograms.

Idealized auto-transiograms are exactly exponential, as shown in Figure 4c. This is decided by the first-order Markovian assumption. Idealized cross-transiograms show three kinds of shapes: exponential, Gaussian, and gamma-featured (i.e., having a single peak close to the origin). From the shapes of idealized cross-transiograms, it is easy to understand the following three situations: if the neighboring structure of two categories occurs randomly in space (which is much less possible in the real world), their experimental cross-transiograms should be gamma-featured; if it occurs irregularly, their experimental cross-transiograms should still be gamma-featured because transiograms as global spatial measures do not reflect local differences; but if the occurrence is periodical or pseudo-periodical in space, their experimental cross-transiograms should typically have hole-effect features. In general, the occurrence of the peaking features on some idealized cross-transiograms implies that the occurrence of peaking features on some experimental cross-transiograms is normal, and such peaking features can be real reflections of spatial heterogeneity of landscapes rather than ill shapes caused by data problems if samples used are not excessively sparse.

2.4. Comparison of experimental and idealized transiograms

Although idealized transiograms are smooth in shape, they are relatively simple because of the implicit assumptions. Some idealized transiograms may approximately fit their corresponding experimental ones, but most may deviate a lot, as demonstrated in Figures 6 and 7. The deviation between an experimental cross-transiogram and its corresponding idealized one is more obvious when a peaking feature occurs. They do fit at initial lag distances nearby the first space step, but have no guarantee to fit at higher lag distances. This means that idealized transiograms are not good enough to serve as transiogram models although they can help explain some features of the experimental ones when available. Although idealized transiograms are seldom directly available, unless there is no data or no sufficient data to estimate experimental transiograms (e.g., sometimes in hydrogeology), it is not recommended to use idealized transiograms derived from expert-guessed TPMs in geostatistical simulations.

Idealized transiograms are not truly continuous, as aforementioned. If they are calculated from one-step TPMs, they have gaps of a single pixel length. If they are calculated from multistep TPMs, they have gaps of multiple pixel lengths. But it is easy to make them continuous by interpolation if the gap is not too large, or even by model fitting given the simplicity of their shapes.

3. Transiogram models with gamma distribution

3.1. Gamma distribution

In probability theory and statistics, gamma distribution is a two-parameter family of continuous probability distributions. It has a scale parameter β (beta) and a shape parameter

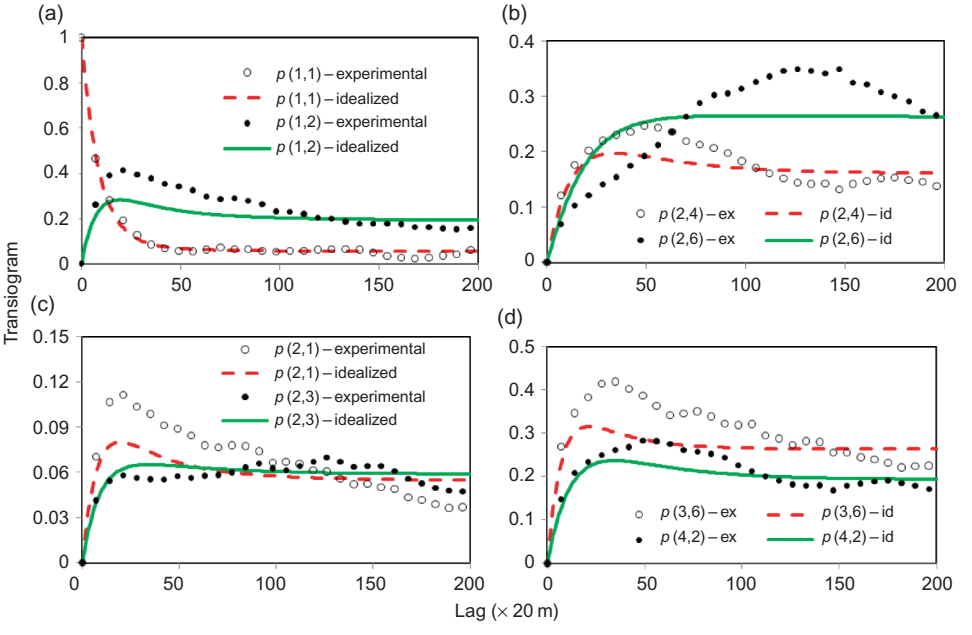

Figure 6. Idealized transiograms and their corresponding experimental transiograms calculated from land cover data.

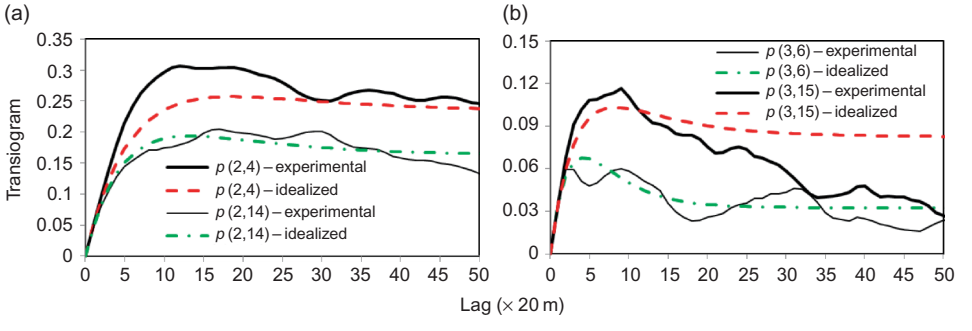

Figure 7. Idealized transiograms and their corresponding experimental transiograms calculated from soil map data.

α (alpha). If α is an integer, then the distribution represents the sum of α independent exponentially distributed random variables, each of which has a mean of β. Gamma distribution (probability density function) is right-skewed (i.e., positively skewed, the right tail is longer) and bounded at zero. Like lognormal distribution, it is an alternative to be considered for variables that seem to be highly skewed.

Gamma distribution has been used as a model in a range of disciplines, such as climatology, where it is a workable model for rainfall, and financial services, where it is used for modeling insurance claims and the size of loan defaults. It is frequently a probability model for waiting times; for instance, in life testing, the waiting time until death is a random variable that is frequently modeled with a gamma distribution (Hogg and Craig 1978). Gamma distributions were fitted to rainfall amounts from different storms (Rice 1995). They were

also used in landscape ecology, for example, to model species abundances (Plotkin and Muller-Landau 2002), and in soil science, for example, to describe soilscape boundary spacings (Burgess and Webster 1984).

The gamma distribution (probability density function) is given as

$$f_{\alpha,\beta}(x) = \frac{1}{\Gamma(\alpha)\beta^{\alpha}} x^{\alpha-1} e^{-\frac{x}{\beta}} \tag{4}$$

where the gamma function $\Gamma(\alpha)$ is defined as

$$\Gamma(\alpha) = \int_0^{\infty} t^{\alpha-1} e^{-t} dt \tag{5}$$

where α is the shape parameter, and β is the scale parameter, that is, the standard deviation of the gamma distribution is proportional to β. In the gamma distribution, x and the parameters α and β must be positive. The mean and variance of the gamma distribution are $\alpha\beta$ and $\alpha\beta^2$, respectively.

The shape of the gamma distribution is very flexible. Some examples of the gamma distribution, scaled up by 5 (i.e., using $x/5$ to replace x in Equation (4), thus changing the function mean to $5\alpha\beta$), are provided in Figure 8. One can see that when the shape parameter α is set to one or less than one, the gamma distribution is a monotonically decreasing curve and looks like an exponential distribution (Figure 8a); when α is greater than one, the gamma distribution becomes a right-skewed distribution curve, and the peak height changes with both parameters (Figure 8b); and when α increases to a large number and β keeps small, the gamma distribution even tends to be normally distributed (Figure 8c).

In this study, what interests us is the flexible right-skewed shape of the gamma distribution when the shape parameter α is greater than one, which is like the peaking features of some experimental cross-transiograms, first increasing to a peak and then flattening out. The difference is that experimental cross-transiograms will gradually flatten to or fluctuate around their respective sills, whereas the gamma distribution gradually approaches to zero after across a peak (Figure 9a). This implies that if we want to use the gamma distribution

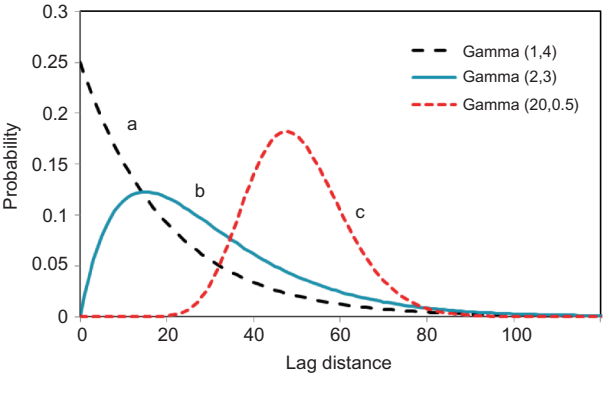

Figure 8. Gamma distributions with different alpha and beta parameters (scaled up by 5), denoted as gamma(α, β) in the legend.

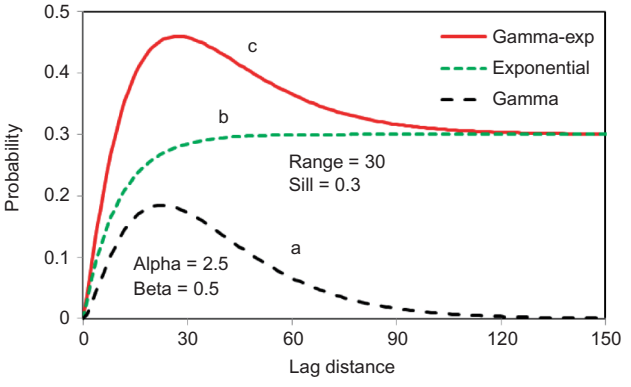

Figure 9. The gamma distribution (a), the exponential model (b), and their additive composite model (c).

to fit experimental transiograms, we have to add a simple function that has a sill to make a composite model. In Figure 9, we show a composite model which adds an exponential function (Figure 9b) to the gamma distribution function. The composite model demonstrates the exact peaking feature we want for cross-transiogram modeling: It first quickly increases to a peak and then flattens out to a stable sill (Figure 9c).

In addition, the cumulative gamma distribution function may also be used independently to fit transiograms or variograms without the peaking or hole-effect features. It is more flexible than the exponential and Gaussian models because the latter are actually special cases of the cumulative gamma distribution. But this is beyond the focus of this study and will not be addressed here.

3.2. Additive gamma-exponential composite model

The additive gamma-exponential composite model, as demonstrated by Figure 9c, may be used to fit some experimental cross-transiograms. The exponential function has been used as a variogram model (Goovaerts 1997) and also used as a transiogram model (Li 2007a, Li *et al*. 2010). The exponential cross-transiogram model can be given as

$$p_{ij}(\mathbf{h}) = c\left[1 - \exp\left(-\frac{3\mathbf{h}}{d}\right)\right] \tag{6}$$

where $\mathbf{h}$ is the lag distance, c is the sill parameter, and d is the parameter of effective range. For transiograms, the sill is theoretically equal to the proportion of the tail category j. Thus, the additive gamma-exponential composite model we propose as a cross-transiogram model can be mathematically expressed as

$$p_{ij}(\mathbf{h}) = c\left[1 - \exp\left(\frac{-3\mathbf{h}}{d}\right) + w\frac{1}{\Gamma(\alpha)\beta^{\alpha}}\left(\frac{\mathbf{h}}{d}\right)^{\alpha-1}\exp\left(\frac{-\mathbf{h}}{\beta d}\right)\right], \alpha > 1, \beta > 0 \tag{7}$$

where $\mathbf{h}$ replaces the x in the gamma distribution of Equation (4) as the lag distance.

This cross-transiogram model is relatively a little complex. It is composed of an exponential cumulative distribution function and a gamma probability density function. It is not like a nested variogram model which is composed of two or more commonly used

variogram models, of which each has its own sill and range parameters. Except for the shape parameter α and the scale parameter β of the gamma distribution function, it has three other parameters, c, d, and w. Here c is still the sill parameter of the exponential function, theoretically equal to the proportion of the tail category j. For the exponential function component, d is the effective range parameter. But for the gamma distribution function component, the use of d is just to put the gamma curve and the exponential curve to the same spatial scale. As to w, it serves as a weight parameter so that we may adjust the weight of the gamma distribution function component in the composite model. Note that there is no explicit range parameter for the whole composite model. With these five parameters, the additive gamma-exponential composite model can easily provide a good fit to the peaking features of experimental cross-transiograms with different peak heights, widths, and even shapes.

In Figures 10 and 11, we display some experimental cross-transiogram examples with different characteristics of the peaking features and their fitted models. Parameters for each transiogram model are provided in its chart. No commonly used variogram models or their nested structures can be used to fit such kind of transiogram shapes. However, by adjusting the five parameters, particularly the three parameters of α, β, and w with the gamma

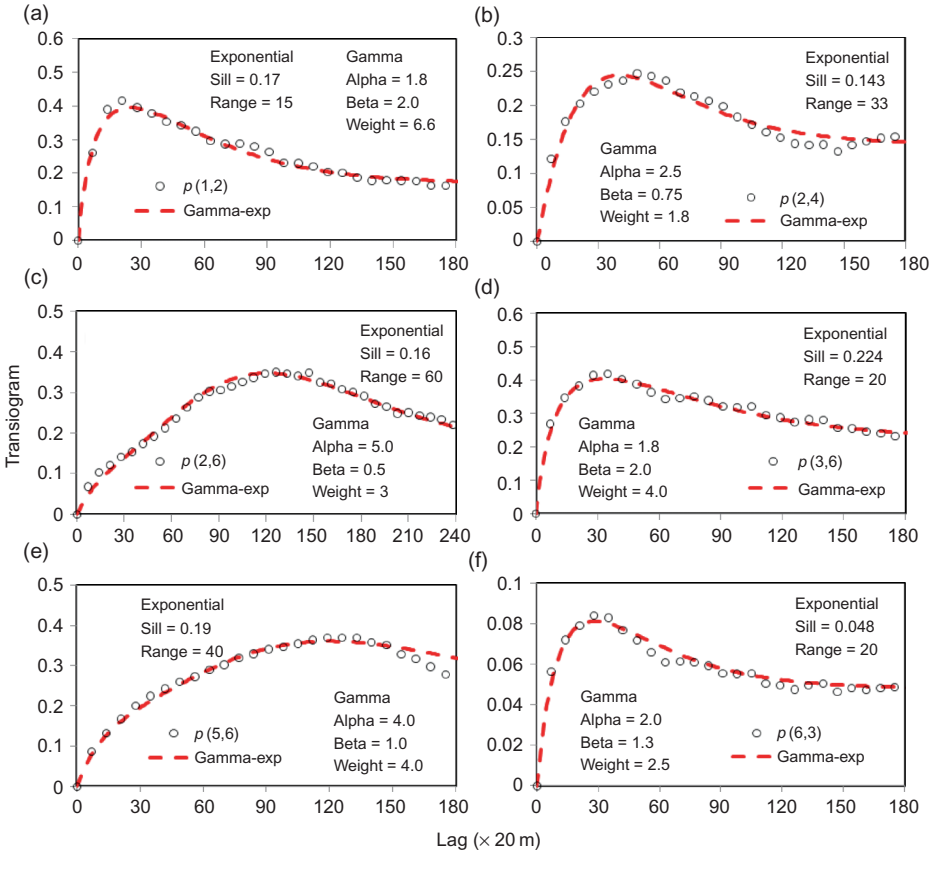

Figure 10. Some experimental cross-transiograms with a peak, estimated from a land cover data set, and their models fitted by the additive gamma-exponential composite model.

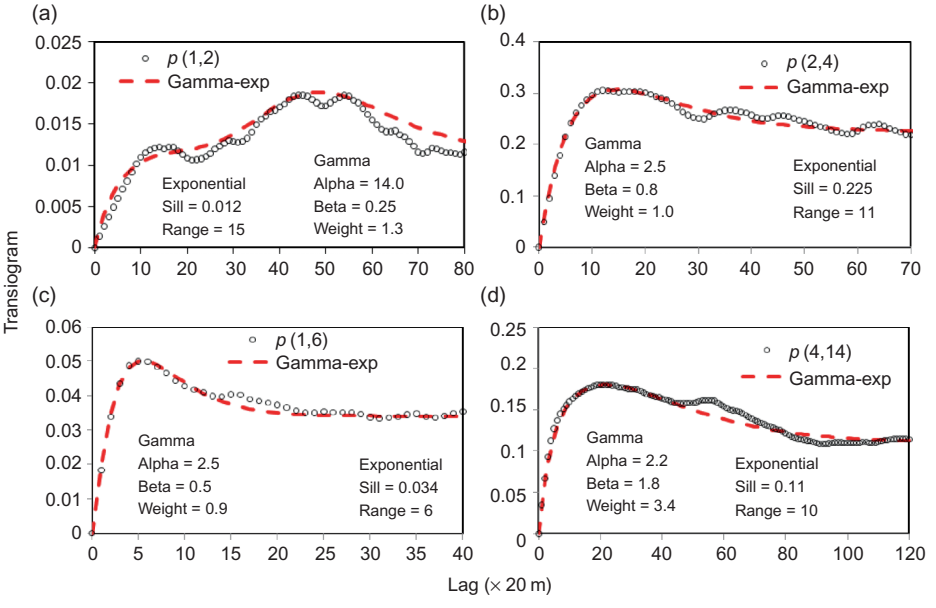

Figure 11. Some experimental cross-transiograms with a peak, estimated from a soil type data set, and their models fitted by the additive gamma-exponential composite model.

distribution function, the proposed additive gamma-exponential composite model can fit all of them very well. Even the peak shapes special as those in Figures 10c and 11a are well fitted. Most of these experimental cross-transiograms have the shape of a quick peak first and then flatten out. This is the special feature that reflects close neighborships. Although the fitting was done manually, one can see that they are almost perfectly fitted. It should be noted that it is far more important to precisely fit the low lag section (i.e., the part close to the origin) than to precisely fit the high lag section, because usually only the low lag section of a transiogram model is used in geostatistical simulations. Our fitting also emphasizes the low lag section, for example, the lag section is less than 60 pixel lengths in the transiogram examples here.

3.3. Other additive composite models with the gamma distribution

In Equation (7), we used an exponential function to work with the gamma distribution function. The Gaussian function and the spherical function, which have been commonly used as basic variogram models (Goovaerts 1997), can also be added to the gamma distribution function to form additive composite models. The additive gamma-Gaussian composite cross-transiogram model and the additive gamma-spherical composite cross-transiogram model can be written as

$$p_{ij}(\mathbf{h}) = c\left[1 - \exp\left(\frac{-3\mathbf{h}^2}{d^2}\right) + w\frac{1}{\Gamma(\alpha)\beta^{\alpha}}\left(\frac{\mathbf{h}}{d}\right)^{\alpha-1}\exp\left(\frac{-\mathbf{h}}{\beta d}\right)\right], \alpha > 1, \beta > 0 \quad (8)$$

and

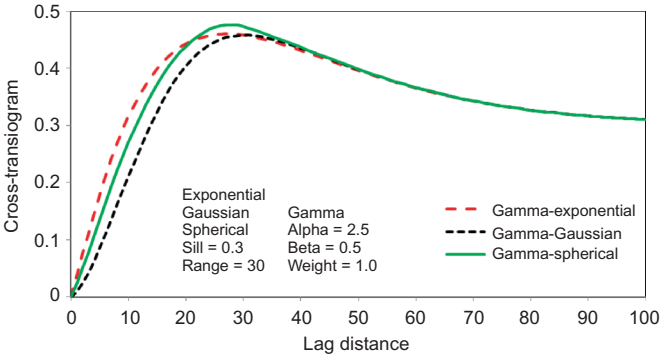

Figure 12. Different gamma-based additive composite models with the same parameter setting.

$$p_{ij}(\mathbf{h}) = \begin{cases} c\left[1.5\dfrac{\mathbf{h}}{d} - 0.5\left(\dfrac{\mathbf{h}}{d}\right)^3 + w\dfrac{1}{\Gamma(\alpha)\beta^\alpha}\left(\dfrac{\mathbf{h}}{d}\right)^{\alpha-1}\exp\left(\dfrac{-\mathbf{h}}{\beta d}\right)\right], & x < d \\ c\left[1 + w\dfrac{1}{\Gamma(\alpha)\beta^\alpha}\left(\dfrac{\mathbf{h}}{d}\right)^{\alpha-1}\exp\left(\dfrac{-\mathbf{h}}{\beta d}\right)\right], & x \geq d \end{cases} \quad ,\alpha > 1, \beta > 0 \tag{9}$$

respectively, where the parameters are the same as those in Equation (7), except that d is the actual range for the spherical function component. These two composite models should generate similar results as those of the additive gamma-exponential composite model. The difference exists in the shapes of the initial section of the cross-transiogram models, that is, the left side of the peak (Figure 12). Similarly, one may consider forming other additive composite models in a similar way. To precisely fit the initial section of experimental cross-transiograms, different additive composite models based on the gamma distribution function may be needed.

4. Comparison with hole-effect transiogram models

In geostatistics, the *hole-effect* refers to the nonmonotonic structures, particularly the alternate peaks and troughs, occurring on variograms (David 1977). If the peaks and troughs attenuate gradually, it is called dampened hole effect. These structures may be bounded by a sill or occur without a sill, be dampened or undampened, and be isotropic or anisotropic (Pyrcz and Deutsch 2003). Studies show that a marked hole effect in variograms is usually the reflection of periodicity or cyclicity on spatial variability, which is a common and legitimate spatial characteristic in geology. Ignoring the nonmonotonic structures may result in unrealistic heterogeneity models that do not reproduce the real patterns of variability (Journel and Huijbregts 1978, Journel and Froidevaux 1982, Jones and Ma 2001, Pyrcz and Deutsch 2003). However, hole effects were often ignored and the spherical model was often fitted through the peaks and troughs of experimental variograms. One reason is the doubt that experimentally observed hole effects may be dubious or sampling artifacts (Journel and Huijbregts 1978), the other reason should be that the mathematical models used to fit hole-effect variograms may not ensure the permissibility requirement of kriging, and thus are regarded as not legitimate (Christakos 1984, Deutsch and Journel 1998).

Whereas the first reason can be true sometimes when samples are very sparse, the second reason, however, seems not a problem in Markov chain geostatistical simulations.

The spatial patterns of landscapes are even more complex due to various natural and human impact factors. Therefore there is nothing strange for hole-effect features to appear in experimental transiograms of landscape categories, as demonstrated in the second section of this paper. Such features provide valuable information concerning the spatial variability of landscapes. Clearly, they must be accounted for, if precise local estimations of landscapes are required.

Figure 13 shows the hole-effect model and the dampened hole-effect model for variogram modeling, provided in Deutsch and Journel (1998). The hole-effect model (Figure 13a) is an adapted cosine function, expressed as

$$\gamma(\mathbf{h}) = c\left[1 - \cos\left(2\pi\frac{\mathbf{h}}{a}\right)\right] \tag{10}$$

where c is the sill and a is the wavelength (i.e., the width of the first peak). This model may be used with the commonly used variogram models such as the spherical model to construct nested models for fitting nonattenuated hole-effect features of experimental variograms. Nonattenuated hole effect is rarely seen in experimental cross-transiograms of multiclass categorical variables, but may appear in binary variables. We will not explore it in this paper. The dampened hole-effect model (Figure 13b) is actually a multiplicative cosine-exponential composite model (Journel and Froidevaux 1982, Hohn 1988, Christakos 1992), which has been used in signal processing (Papoulis 1977). Its characteristics were explored by Ma and Jones (2001) in fitting hole-effect indicator variograms.

The dampened hole-effect model, that is, the multiplicative cosine-exponential composite model, can be directly used as a transiogram model to fit experimental cross-transiograms with similar hole-effect features. As a cross-transiogram model, the multiplicative cosine-exponential composite model is given as follows:

$$p_{ij}(\mathbf{h}) = c\left[1 - \exp\left(-\frac{3\mathbf{h}}{d}\right)\cos\left(2\pi\frac{\mathbf{h}}{a}\right)\right] \tag{11}$$

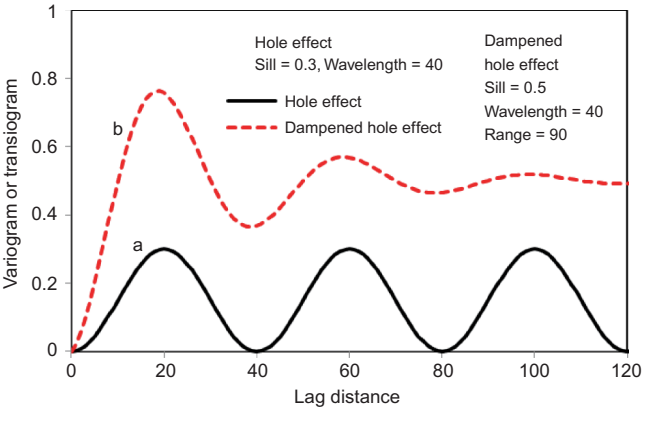

Figure 13. Typical hole-effect models: (a) hole-effect model; (b) dampened hole-effect model.

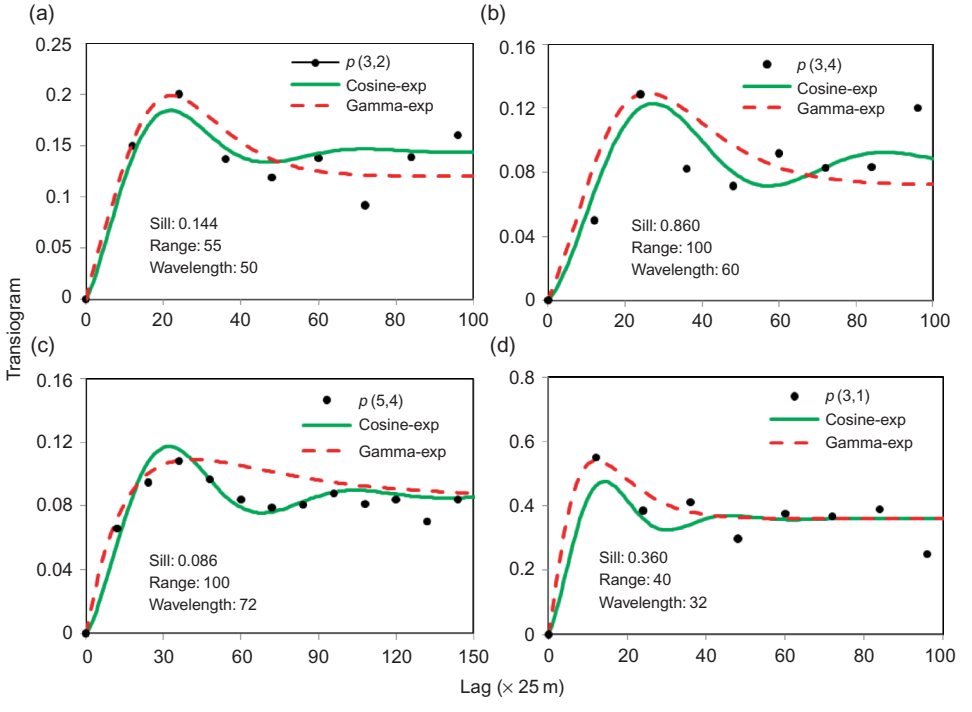

Figure 14. Fitting experimental cross-transiograms using the multiplicative cosine-exponential composite models and the additive gamma-exponential composite models. Parameters are for models fitted using the multiplicative cosine-exponential composite model.

where **h** is the lag distance, c is the sill, d is the effective range, and a is the wavelength of the cosine function. Since the hole effect, that is, the alternate peaks and troughs appearing on real experimental variograms or transiograms, is rarely regular, it is actually difficult to fit a series of peaks and troughs. Considering the useful part of a transiogram model for simulation is just the low lag section, we aim to fit only the first peak and trough of experimental cross-transiograms using this composite model.

Figure 14 shows some experimental cross-transiograms from a small sparse soil data set, and manually fitted transiogram models using the multiplicative cosine-exponential composite model and the additive gamma-exponential composite model. It can be seen that the composite hole-effect model may provide an approximate fit to some experimental cross-transiograms. The transiogram models in Figure 14a and c are all good fits to the first pair of peaks and troughs of experimental transiograms. Although the gamma-exponential composite model is more powerful in fitting the first peak in experimental transiograms, it cannot fit any troughs (see Figure 14c). However, if there is not any clear trough immediately following the first peak, the composite hole-effect model usually cannot work well, because it is difficult to ensure the required height or width of the first peak, at the same time avoiding the following trough in transiogram models (see Figure 14d). Under this situation, it is better to use gamma-based composite models.

In Figure 15, we compare the fitting effectiveness of the multiplicative cosine-exponential composite model and the additive gamma-exponential composite model with some experimental cross-transiograms estimated from large data sets. Here all model fitting is performed manually by trial and error. It can be seen that if there is only a single peak

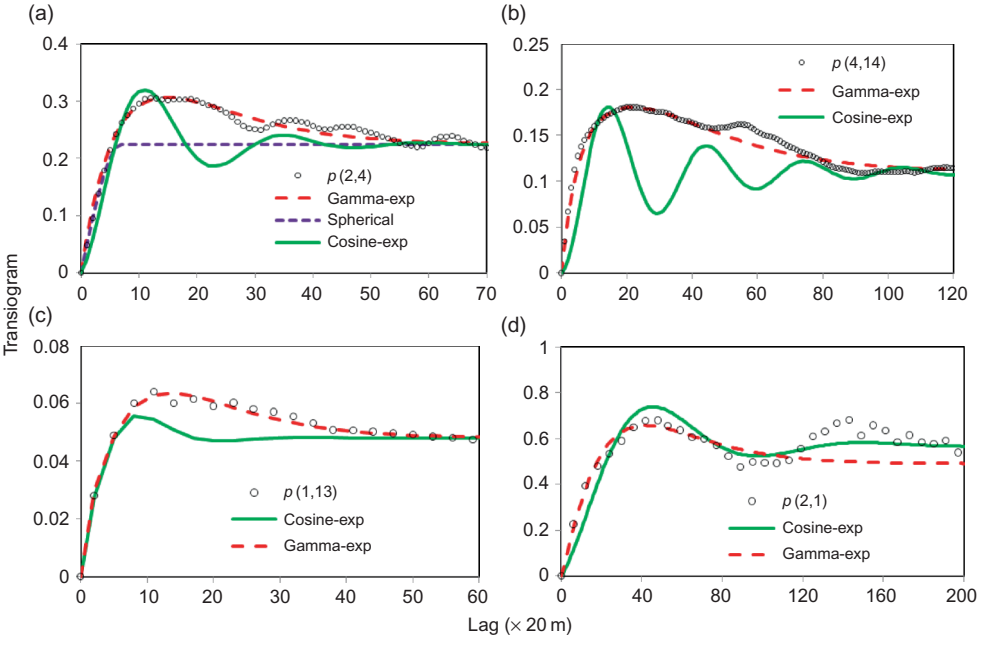

Figure 15. Comparison of the additive gamma-exponential composite model and the multiplicative cosine-exponential composite model in fitting experimental cross-transiorgams.

without apparent troughs, the cosine-exponential model is generally improper, whereas the gamma-exponential model works almost perfectly (see Figure 15a–c). The simple spherical model may fit at the root part but is unacceptable here due to its neglect of the peak (Figure 15a). Sometimes even if there is a series of peaks and troughs, the cosine-exponential model still has difficulty to effectively fit the shape of the first peak, as shown in Figure 15d where the experimental cross-transiogram is from a binary data set. Under this situation, if one just wants to use the low lag section of the transiogram model, using the gamma-exponential model is still a better choice because it is sufficiently flexible to provide a better fit to the first peak (Figure 15d).

Ma and Jones (2001) also provided two other cosine-based composite variogram models with attenuating hole effects. One is the multiplicative cosine-Gaussian composite model, which is written here for transiogram modeling as

$$p_{ij}(\mathbf{h}) = c\left[1 - \exp\left(-\frac{3\mathbf{h}^2}{d^2}\right)\cos\left(2\pi\frac{\mathbf{h}}{a}\right)\right], \tag{12}$$

where the parameters are as in the model (Equation (11)). The other one is the multiplicative cosine-spherical composite model, which was unfortunately mistakenly written (see Ma and Jones 2001, p. 639). The correct form of the model for transiogram modeling is given here as

$$p_{ij}(\mathbf{h}) = \begin{cases} c\left[1 - \left(1 - \left(1.5\frac{\mathbf{h}}{d} - 0.5\left(\frac{\mathbf{h}}{d}\right)^3\right)\right)\cos\left(2\pi\frac{\mathbf{h}}{a}\right)\right], & x < d \\ c, & x \geq d \end{cases} \tag{13}$$

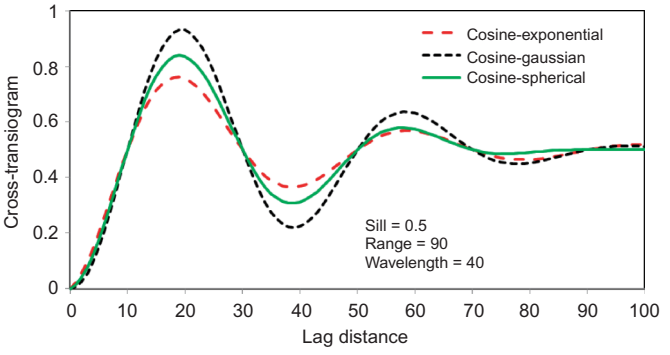

Figure 16. Different cosine-based multiplicative composite models with the same parameter setting.

where the parameters are as in the model (Equation (11)), except that d here is the actual range. These cosine-based composite models attenuate the sinusoidal amplitudes with increasing lag distance. However, their amplitudes differ. Given the same parameter values, the peak heights of the cosine-Gaussian model are highest, those of the cosine-exponential model are lowest, and the cosine-spherical model generally loses cyclicity faster than others (Figure 16). Similar to model (11), models (12) and (13) can be used to fit experimental cross-transiograms with hole effects. The main limitations for cosine-based multiplicative composite models are that it is often difficult to adjust their peak heights and widths to desirable conditions, and the Gaussian-shaped root sections caused by the cosine function (see Figure 16) often do not fit experimental transiograms (or variograms) well. These unidealities can also be seen from fitting cases in Ma and Jones (2001). However, to fit more than one peak and trough in experimental transiograms, we need these composite hole-effect models.

5. Conclusions

The features of transiograms of spatial categories, particularly frequent neighboring category pairs, are demonstrated. Some experimental cross-transiograms indicate apparently a peak at low lag distances. The peak is usually too much above the sill of the cross-transiogram to ignore. It often simply flattens out without a following trough, but sometimes may be followed by some, usually attenuating, troughs and peaks. Whereas the latter situation may be caused by the cyclic occurrence of neighboring structures in landscape categories, similar as that found in geology where spatial patterns may be more regular, the former situation should result from the pseudo-random distribution of neighboring structures, which is common in natural landscapes. This can be proved by the corresponding idealized transiograms calculated from one-step TPMs. Existing hole-effect models are not flexible enough to effectively fit these kinds of cross-transiograms.

We propose using the gamma distribution function and the commonly used variogram (or transiogram) models to form additive composite models for fitting such kinds of experimental transiograms, and provide three such models. Fitting cases of experimental cross-transiograms of landscape data (i.e, soil types and land cover classes) show that the additive gamma-exponential composite model works very well and may fit closely the single-peak features. Apparently, the proposed composite models are also applicable to fitting experimental indicator variograms with similar features. Although it has five parameters to set, model fitting can be performed manually by trial and error. If a software tool

with moving buttons of parameters (mainly the alpha, beta, and weight parameters) could be developed, the parameter-setting burden would be released. An unideality of gamma-based composite models is that we cannot set the range parameter of a whole composite model because it is not explicit. We also reintroduce the composite hole-effect models proposed for variogram modeling by earlier researchers (see Ma and Jones 2001) and test them on experimental cross-transiograms. It is found that composite hole-effect models have some obvious limitations in effectively fitting the peak shapes of experimental cross-transiograms of neighboring categories.

On the basis of the investigations made in this study, we make the following recommendations in modeling the peaking features of transiograms: (1) if an experimental cross-transiogram is single-peaked (i.e., no other apparent peaks and troughs), use gamma-based additive composite models; (2) if one just wants a better fit to the first peak, use gamma-based additive composite models rather than hole-effect models; (3) if one needs to fit at least the first pair of regular peaks and troughs, use cosine-based multiplicative composite hole-effect models, which often can do a good job. However, to fit multiple peaks and troughs with irregular sizes, it is better to use nonparametric methods (Shapiro and Botha 1991, Genton and Gorsich 2002). In addition, it should be pointed out that for peaks or troughs located far away from the origin it is not only difficult but also useless to fit them.

References

Almeida, C.M., *et al*., 2008. Using neural networks and cellular automata for modelling intra-urban land-use dynamics. *International Journal of Geographical Information Science*, 22, 943–963.

Burgess, T.M. and Webster, R., 1984. Optimal sampling strategies for mapping soil types. I. Distribution of boundary spacings. *Journal of Soil Science*, 35, 641–654.

Carle, S.F. and Fogg, G.E., 1996. Transition probability-based indicator geostatistics. *Mathematical Geology*, 28, 453–477.

Christakos, G., 1984. On the problem of permissible covariance and variogram models. *Water Resources Research*, 20, 251–265.

Christakos, G., 1992. *Random field models in earth sciences*. San Diego, CA: Academic Press, 474 p.

David, M., 1977. *Geostatistical ore reserve estimation*. New York: Elsevier, 364 p.

Dendoncker, N., Schmit, C., and Rounsevell, M., 2008. Exploring spatial data uncertainties in land-use change scenarios. *International Journal of Geographical Information Science*, 22, 1013–1030.

Deutsch, C.V. and Journel, A.G., 1998. *GSLIB: Geostatistics software library and user's guide*. 2nd ed. New York: Oxford University Press.

Dietzel, C., *et al*., 2005. Spatio-temporal dynamics in California's Central Valley: empirical links to urban theory. *International Journal of Geographical Information Science*, 19, 175–195.

Geertman, S., Hagoort, M., and Ottens, H., 2007. Spatial-temporal specific neighbourhood rules for cellular automata land-use modeling. *International Journal of Geographical Information Science*, 21, 547–568.

Genton, M.G. and Gorsich, D.J., 2002. Nonparametric variogram and covariogram estimation with Fourier–Bessel matrices. *Computational Statistics & Data Analysis*, 41, 47–57.

Goovaerts, P., 1997. *Geostatistics for natural resources evaluation*. New York: Oxford University Press, 483 p.

Haines-Young, R. and Chopping, M., 1996. Quantifying landscape structure: a review of landscape indices and their application to forested landscapes. *Progress in Physical Geography*, 20, 418–445.

Hobbs, R.J. and McIntyre, S., 2004. Categorizing Australian landscapes as an aid to assessing the generality of landscape management guidelines. *Global Ecology and Biogeography*, 14, 1–15.

Hogg, R.V. and Craig, A.T., 1978. *Introduction to mathematical statistics*. 4th ed. New York: Macmillan.

Hohn, M.E., 1988. *Geostatistics and petroleum geology*. New York: Van Nostrand Reinhold, 264 p.
Jones, T.A. and Ma, Y.Z., 2001. Teacher's aide: geologic characteristics of hole-effect variograms calculated from lithology-indicator variables. *Mathematical Geology*, 33, 615–629.
Journel, A.G. and Froidevaux, R., 1982. Anisotropic hole-effect modeling. *Mathematical Geology*, 14, 217–239.
Journel, A.G. and Huijbregts, CH.J., 1978. *Mining geostatistics*. New York: Academic Press, 600 p.
Li, W., 2006. Transiogram: a spatial relationship measure for categorical data. *International Journal of Geographical Information Science*, 20, 693–699.
Li, W., 2007a. Transiograms for characterizing spatial variability of soil classes. *Soil Science Society of American Journal*, 71, 881–893.
Li, W., 2007b. Markov chain random fields for estimation of categorical variables. *Mathematical Geology*, 39, 321–335.
Li, W., *et al*., 2010. Estimating threshold-exceeding probability maps of continuous environmental variables with Markov chain random fields. *Stochastic Environmental Research and Risk Assessment*, 24, 1113–1126.
Li, H. and Reynolds, J.F., 1993a. On definition and quantification of heterogeneity. *Oikos*, 73, 280–284.
Li, H. and Reynolds, J.F., 1993b. A new contagion index to quantify spatial patterns of landscapes. *Landscape Ecology*, 8, 155–162.
Li, W. and Zhang, C., 2007. A random-path Markov chain algorithm for simulating categorical soil variables from random point samples. *Soil Science Society of American Journal*, 71, 656–668.
Li, W. and Zhang, C., 2010. Linear interpolation and joint model fitting of experimental transiograms for Markov chain simulation of categorical spatial variables. *International Journal of Geographical Information Science*, 24, 821–839.
Li, W. and Zhang, C., 2011. A Markov chain geostatistical framework for land-cover classification with spatial uncertainty assessment based on expert-interpreted pixels from remotely sensed imagery. *IEEE Transactions on Geoscience and Remote Sensing*, 49, 2983–2992.
Lou, J., 1993. *Konditionale Markovsimulation 2-dimensionaler geologischer problem*. Berliner Geowissenschaftliche Abhandlungen, Reihe D, Band 4, Berlin.
Ma, Y.Z. and Jones, T.A., 2001. Teacher's aide: modeling hole-effect variograms of lithology-indicator variables. *Mathematical Geology*, 33, 631–648.
McGarigal, K. and Marks, B.J., 1995. *FRAGSTATS: spatial pattern analysis program for quantifying landscape structure*. Portland, OR: USDA, Forest Service, Pacific Northwest Research Station, Gen. Tech. Rep. PNW–GTR–351, 122 p.
O'Neill, R.V., *et al*., 1988. Indices of landscape pattern. *Landscape Ecology*, 1, 153–162.
Palmer, J.F., 2004. Using spatial metrics to predict scenic perception in a changing landscape: Dennis, Massachusetts. *Landscape and Urban Planning*, 69, 201–218.
Papoulis, A., 1977. *Signal analysis*. New York: McGraw-Hill, 431 p.
Pickett, S.T.A. and Cadenasso, M.L., 1995. Landscape ecology: spatial heterogeneity in ecological systems. *Science*, 269, 331–334.
Pijanowski, B.C., *et al*., 2005. Calibrating a neural network-based urban change model for two metropolitan areas of the Upper Midwest of the United States. *International Journal of Geographical Information Science*, 19, 197–215.
Plotkin, J.B. and Muller-Landau, H.C., 2002. Sampling the species composition of a landscape. *Ecology*, 83, 3344–3356.
Pontius, G.R. and Malanson, J., 2005. Comparison of the structure and accuracy of two land change models. *International Journal of Geographical Information Science*, 19, 243–265.
Pyrcz, M. and Deutsch, C., 2003. The whole story on the hole effect. *Geostatistical Association of Australasia Newsletter*, 18, 3–5.
Rice, J., 1995. *Mathematical statistics and data analysis*. 2nd ed. Belmont, CA: Duxbury Press, 244 p.
Riitters, K.H., *et al*., 1995. A factor analysis of landscape pattern and structure indices. *Landscape Ecology*, 10, 23–39.
Ritzi, R.W., 2000. Behavior of indicator variograms and transition probabilities in relation to the variance in lengths of hydrofacies. *Water Resources Research*, 36, 3375–3381.
Robbins, P., 2001. Fixed categories in a portable landscape: the causes and consequences of land-cover categorization. *Environment and Planning A*, 33, 161–179.

Shapiro, A. and Botha, J.D., 1991. Variogram fitting with a general class of conditionally nonnegative definite functions. *Computational Statistics & Data Analysis*, 11, 87–96.

Turner, M.G., 1989. Landscape ecology: the effect of pattern on process. *Annual Review of Ecology and Systematics*, 20, 171–197.

Wu, J., *et al*., 2002. Empirical patterns of the effects of changing scale on landscape metrics. *Landscape Ecology*, 17, 761–782.